Journal of Applied Mechanics and Technical Physics, Vol. 47, No. 3, pp. 419–425, 2006

NUMERICAL MODELING OF THE SHEARING OF IRRADIATED FUEL ASSEMBLIES

Yu. P. Meshcheryakov

UDC 539.3

The stress–strain state of layered bodies is studied numerically taking into account features of the loading devices used in the technological shearing processes of irradiated fuel assemblies. The effect of the localization of the hold-down clamp on the shear stress intensity and the shear stress value is studied. The dependence of the stress–strain state of the layers on the value of the gap between the blades is obtained. It is shown that the nature of the failure changes in the process of wearing of the shear blade edges.

Key words: *shearing, numerical modeling, layered bodies, fuel assembly.*

Introduction. The problem of nuclear waste disposal includes a complex of technological processes, one of which is the shearing of irradiated fuel assemblies. Before shearing, the fuel assembly is subjected to machine working, after which the irradiated fuel assembly can be considered a layered compact. For shearing, the compact is loaded by two blades and a hold-down clamp (Fig. 1). The shearing effectiveness depends on a number of factors: the localization of the hold-down clamp, the wear of the blade edges, the thickness and number of the layers etc.

In the work described here, the stress–strain state of layered compacts was studied numerically as a function of the factors listed above using the model of linear elasticity. The problem was solved by a finite element method ignoring mass forces. Features of the formulation of the problem are statically determined contact boundaries, whose presence considerably reduces the choice of methods for obtaining a stationary solution. The relaxation method was used. Convergence to the stationary solution was ensured by introducing artificial dissipation of energy.

1. Formulation of the Problem. In the theory of linear elasticity, a plane stress–strain state is described by the system of equations [1]

$$\frac{\partial \sigma_{11}}{\partial x} + \frac{\partial \sigma_{12}}{\partial y} = \rho \frac{\partial^2 u}{\partial t^2}, \qquad \frac{\partial \sigma_{21}}{\partial x} + \frac{\partial \sigma_{22}}{\partial y} = \rho \frac{\partial^2 v}{\partial t^2},$$

$$\sigma_{11} = \lambda \operatorname{div} \boldsymbol{u} + 2\mu \frac{\partial u}{\partial x}, \qquad \sigma_{22} = \lambda \operatorname{div} \boldsymbol{u} + 2\mu \frac{\partial v}{\partial y}, \qquad \sigma_{12} = \mu\Big(\frac{\partial u}{\partial y} + \frac{\partial v}{\partial x}\Big).$$

Here ρ is the density, λ and μ are Lamé constants, σ_{ij} $(i = 1, 2;\ j = 1, 2)$ are the stress tensor components, u and v are the displacement vector components, and $\boldsymbol{u}$ is the displacement vector. The Lamé constants are linked to Young's modulus E and Poisson's constant ν by the relation

$$\lambda = \frac{E\nu}{(1+\nu)(1-2\nu)}, \qquad \mu = \frac{E}{2(1+\nu)}.$$

A flattened fuel assembly was simulated by a flat compact consisting of several steel plates. The loading diagram is shown in Fig. 1. The hold-down clamp was treated as an absolutely rigid wall, the fixed blade as a fixed-base plate, and the moving blade as a plate loaded by external pressure.

Design-Technological Branch, Lavrent'ev Institute of Hydrodynamics, Siberian Division, Russian Academy of Sciences, Novosibirsk 630090; ura@kti-git.nsc.ru. Translated from Prikladnaya Mekhanika i Tekhnicheskaya Fizika, Vol. 47, No. 3, pp. 134–140, May–June, 2006. Original article submitted July 28, 2005.

0021-8944/06/4703-0419 © 2006 Springer Science + Business Media, Inc.

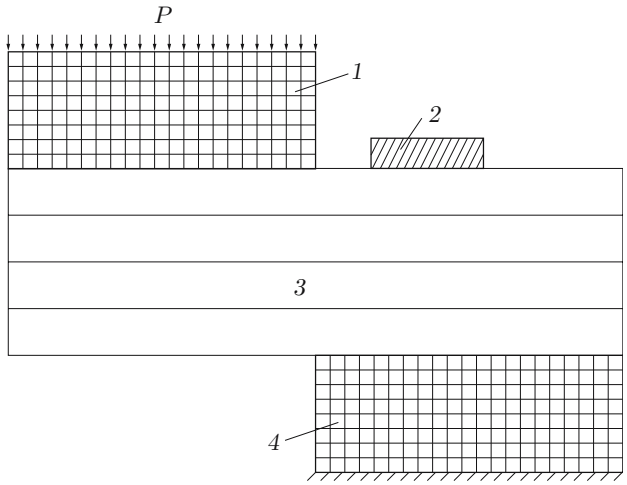

Fig. 1. Diagram of loading of a multilayer compact: 1) moving blade; 2) hold-down clamp; 3) assembly of metal plates; 4) fixed blade.

The following initial data and constants were adopted: elastic modulus $E = 2.1 \times 10^5$ MPa, Poisson's constant $\nu = 0.3$, density of steel $\rho = 7.85 \cdot 10^3$ kg/m^3, displacement vector $\boldsymbol{u}|_{t=0} = 0$, stress-tensor components $\sigma_{ij}|_{t=0} = 0$ $(i = 1, 2;\ j = 1, 2)$.

The following boundary conditions were specified:

1) external load on the moving blade $P = 150$ MPa;

2) $u^n|_{\Gamma^+} = u^n|_{\Gamma^-}$ and $\sigma^n|_{\Gamma^+} = \sigma^n|_{\Gamma^-}$ on the contact boundaries,;

3) $u^n = 0$ on the rigid wall;

4) $\boldsymbol{u} = 0$ on the fixed base;

5) $P = 0$ on the free boundaries.

2. Finite-Element Model. The finite-element model was constructed using the Jourden variational principle [2] for a continuous medium:

$$\int\limits_{\Omega} (\rho\alpha^k - \sigma^{kj}_{,j})\delta u_k \, d\Omega = 0, \qquad k = 1, 2, \quad j = 1, 2. \tag{2.1}$$

Here Ω is the two-dimensional region studied, u_k and α^k are the velocity and acceleration components, respectively; and σ^{kj} $(k = 1, 2,\ j = 1, 2)$ is the symmetric stress tensor.

Integrating by parts and using the Ostrogradskii–Gauss theorem, we write equality (2.1) as

$$\int\limits_{\Omega} \rho\alpha^k \, \delta u_k \, d\Omega = \int\limits_{L} \sigma^{kj} n_j \, \delta u_k \, dl - \int\limits_{\Omega} \sigma^{kj} \, \delta e_{kj} \, d\Omega, \tag{2.2}$$

where e_{kj} is the strain rate tensor and n_j is the component of the normal vector to the boundary of region L.

By means of triangulation, the region Ω was partitioned into triangular elements Ω^e. Approximation of u_k on the element Ω^e was implemented using piecewise linear basis functions $\varphi^e_i(\boldsymbol{X})$:

$$\varphi^e_i = \begin{cases} a^e_i + b^{ej}_i x_j, & \boldsymbol{X} \in \Omega^e, \\ 0, & \boldsymbol{X} \notin \Omega^e, \end{cases} \qquad (i = \overline{1, 3}).$$

Here $\boldsymbol{X}$ is the vector of the point with coordinates (x_1, x_2). In this case,

$$\varphi^e_i(\boldsymbol{X}^n) = \begin{cases} 1, & i = n, \\ 0, & i \neq n \end{cases}$$

(i, n is the local numbering of the finite-element nodes and $\boldsymbol{X}^n$ is the radius vector of the nth vertex of the element). Using the transformation of the vector $\boldsymbol{A}$

$$\tilde{\Phi}^e \boldsymbol{A} = A^i \varphi^e_i \qquad (i = \overline{1, 3}),$$

where A^i are the values of the function at the nodes of the element, we write the components of the velocity, acceleration, and strain rate tensor as

$$u_k(\boldsymbol{X},t)=\sum_e \tilde{\Phi}^e_\alpha(\boldsymbol{X})U^\alpha_k(t)=\sum_e \Phi^e_{\beta k}(\boldsymbol{X})U^\beta(t),$$

$$a_k(\boldsymbol{X},t)=\sum_e \tilde{\Phi}^e_\alpha(\boldsymbol{X})\dot{U}^\alpha_k(t)=\sum_e \Phi^e_{\beta k}(\boldsymbol{X})\dot{U}^\beta(t), \tag{2.3}$$

$$e_{kj}(\boldsymbol{X},t)=\sum_e \left(\Phi^e_{\beta k,j}(\boldsymbol{X})+\Phi^e_{\beta j,k}(\boldsymbol{X})\right)\frac{U^\beta(t)}{2}=\sum_e \Psi^e_{\beta kj}(\boldsymbol{X})U^\beta(t).$$

Here $\alpha=\overline{1,N^e}$, $\beta=\overline{1,2N}$, t is the time coordinate, N^e is the number of elements, N is the number of nodes, and $U^\beta(t)$ is the global velocity component at the mesh nodes.

Using (2.2) and (2.3) and taking into account that the variations over the velocities are independent, it is easy to derive the following equation:

$$M_{\alpha\beta}\dot{U}^\beta=P_\alpha-K_\alpha,\qquad \alpha=\overline{1,2N},\quad \beta=\overline{1,2N}, \tag{2.4}$$

where

$$M_{\alpha\beta}=\sum_e\int\limits_{\Omega^e}\rho\Phi^e_{\beta k}\Phi^e_{\alpha k}\,d\Omega; \tag{2.5}$$

$$P_\alpha=\sum_e\int\limits_{L^e}\sigma^{kj}n_j\Phi^e_{\alpha k}\,dl,\qquad K_\alpha=\sum_e\int\limits_{\Omega^e}\sigma^{kj}\Psi^e_{kj\alpha}\,d\Omega,\qquad k=1,2,\quad j=1,2.$$

The problem reduces to solving the system of differential equations (2.4) for $U^\beta(t)$. Dynamic boundary conditions are incorporated in the first term of the right side of (2.2), and kinematic conditions are taken into account by correcting the external- and internal-load vectors P_α and K_α [3]. The condition imposed on the pressure was used as the dynamic boundary conditions. At the initial time ($t=0$), we set

$$U^\beta=0,\qquad \beta=\overline{1,2N}.$$

Applying the finite-difference operator over the time coordinate to Eq. (2.4), we obtain a vector recursive equation to determine the nodal velocities with a stepwise increase in time by the value τ determined from the loading stability condition:

$$\boldsymbol{U}^{n+1}=\boldsymbol{U}^n+M^{-1}(\boldsymbol{P}^n-\boldsymbol{K}^n)\tau,\qquad \boldsymbol{U}^0=0. \tag{2.6}$$

The matched matrix of masses (2.5) was replaced by its diagonal approximation [4]

$$M_{\alpha\beta}=\begin{cases}\dfrac{1}{3}\displaystyle\sum_r\rho_0\Delta^r_0, & \alpha=\beta,\\ 0, & \alpha\neq\beta,\end{cases}$$

where ρ_0 is the initial density and Δ^r_0 is the initial volume of the element; the summation is performed over elements that contain the corresponding mesh node. The resulting equation (2.6) describes plane motion of a finite-element medium with a piecewise constant distribution of rigidity properties and a point distribution of inertia properties. The stress tensor was calculated at the beginning of each time step.

A stationary solution was obtained by inclusion of synthetic dissipation of energy in the computation algorithm by multiplying the velocity $\boldsymbol{U}^n$ by the coefficient $\omega<1$. In the calculations, we set $\omega=0.99$.

3. Calculation Results. Numerical calculations were performed for an assembly of metal plates with dimensions corresponding to a VVÉP fuel assembly after flattening: length $L=500$ mm, width $W=240$ mm, and thickness $h=30$ mm. The number of plates in the assembly was varied from one to three. We calculated the maximum levels of shear stresses in the assembly $(\sigma_i)^{\max}_a$ and blades $(\sigma_i)^{\max}_k$ and the maximum shear stress $\tau^{\max}_s$ in the section of the assembly by the plane that passes between the blades perpendicular to its surface, i.e., in the plane of the section in which the material undergoes shear and failure in the process considered.

TABLE 1

Maximum Stresses for Various Localizations of the Hold-Down Clamp

Calculation version	$(\sigma_i)_a^{\max}$, MPa	$(\sigma_i)_k^{\max}$, MPa	$\tau_s^{\max}$, MPa
1	2200	2400	1900
2	2100	2800	1100
3	2100	3100	570

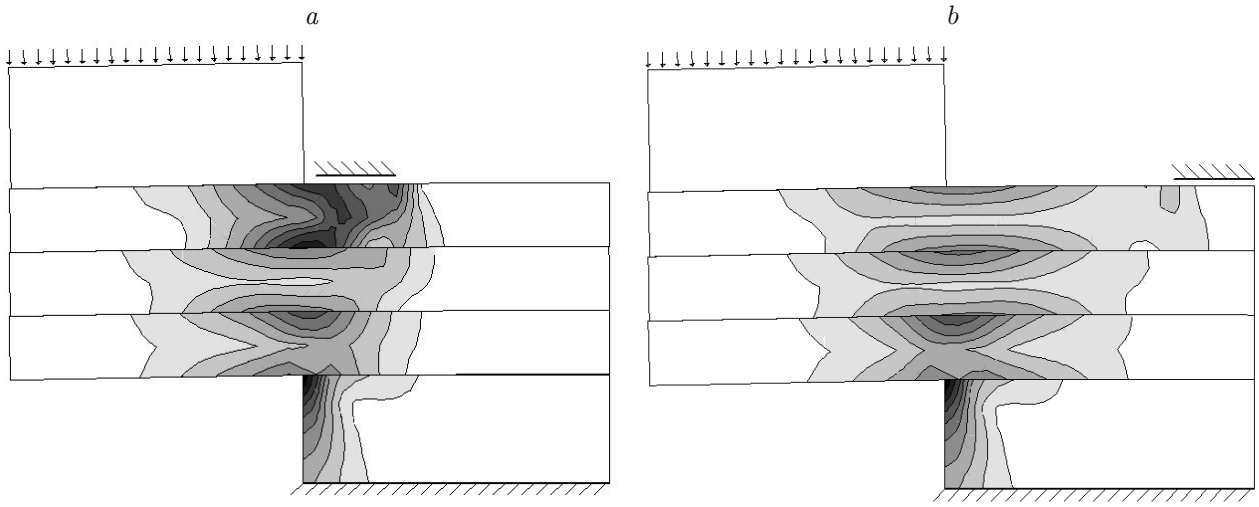

Fig. 2. Shear stress isolines in the cases where the hold-down clamp is located at the edge of the upper blade (a) and at a large distance from it (b).

3.1. *Effect of the Localization of the Hold-Down Clamp on the Stress–Strain State of the Assembly.* The effect of the localization of the hold-down clamp was studied on an assembly consisting of three layers. Three versions of localization of the hold-down clamp were considered. In the first version,the hold-down clamp was located in immediate proximity to the edge of the moving blade, and in the second version and third version, it was located at distances of 0.025 m and 0.05 m, respectively from the blade edge. The calculation results are given in Table 1. From Table 1 it follows that in the case of a large enough distance between the hold-down clamp and the blade edge, the stress–strain state more closely corresponds to the stress–strain state in the case of uniaxial tension rather than in the case of shear.

A comparative analysis of the stress levels shows that the location of the hold-down clamp in immediate proximity to the blade has two advantages: 1) decreased ultimate load on the blade edges, facilitating a decrease in their wearing; 2) increased shear stresses in the assembly, especially shear stresses. The shear stresses become almost equal to the maximum shear stresses, and, therefore, the yield line is almost parallel to the plane normal to the surface of the assembly, which leads to more effective failure of the material.

The shear stress isolines are given in Fig. 2. Dark color corresponds to higher stress levels. From the stress distribution pattern shown in Fig. 2a, it follows that the fixed lower blade is loaded to a greater extent than the upper blade; the most loaded region is the upper layer of the assembly and the least loaded regions are the upper blade and the middle part of the assembly. When the hold-down clamp is at a considerable distance from the edge of the moving blade (Fig. 2b), the lower layer and the fixed blade are the maximum loaded regions. The stress concentration in the assembly is lower than that in the case corresponding to Fig. 2a. When the hold-down clamp takes an intermediate position, the maximum stresses in the layers of the assembly differ insignificantly.

3.2. *Effect of the Wearing of the Blade Edges on the Stress–Strain State of the Assembly.* In the modeling of the wearing of the blade edges, their sections were specified in the form of trapezoids (Fig. 3).

The stress–strain state of a three-layer assembly and a layer consisting of one plate was considered for the gap between the edges of the blades varying from 2 to 10 mm. The loading of the layer consisting of one thin plate

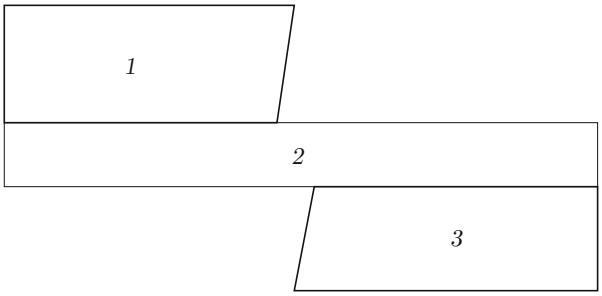

Fig. 3. Diagram of shearing using bevel-edged blades: 1) moving blade; 2) metal plate; 3) fixed blade.

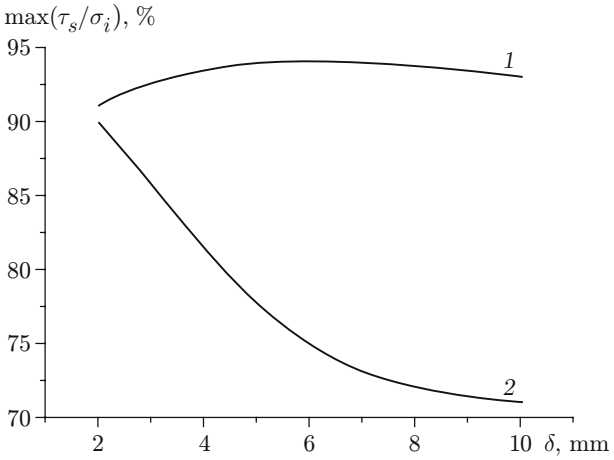

Fig. 4. Maximum ratios of the shear stress to the internal shear: curves 1 and 2 refer to the three-layer assembly and single plate, respectively.

corresponds to the final stage of shearing of the layered assembly. The thickness of the single plate was 10 mm. In all versions of the calculation, the hold-down clamp was placed in immediate proximity to the edge of the upper blade. The calculation results are presented in Fig. 4. It is evident that the dependences of the stress–strain state of the three-layer assembly and that of the single plate on the value of the gap δ between the edges of the blades differ qualitatively. As the gap increases, the ratio of the shear stress τ_s to the shear stress intensity σ_i in the case of a single plate decreases considerably. Thus, similarly to the case of remote location of the hold-down clamp, in the case of a large value of the gap, the stress–strain state of the single plate more closely corresponds to the stress–strain state that arises in the material under uniaxial tension rather than under shear. The dependence of the stress–strain state of the assembly on the distance between the edges of the blades in the examined range of the gap values is weak and corresponds to shearing conditions. It should be noted that the optimal conditions for shearing occur when the gap is small (3–4 mm) since the ratio of the shear stress to the internal shear is maximal in this case.

An analysis of the results leads to the conclusion that the wearing of the blade edges has a weak effect on the shearing effectiveness of the first layers but considerably reduces the shearing effectiveness of layered materials in the final stage of the process (Fig. 5). A comparison of the plate deflections in Fig. 5a and b shows that for $\delta = 10$ mm, the plate has a greater deflection. In practice, it is difficult to ensure considerable deflections required to achieve stress levels sufficient for shearing, which limits the use of worn-edged blades.

3.3. *Effect of the Number of Layers on the Stress–Strain State of the Assembly.* An assembly of total thickness 30 mm consisting of layers of identical thickness was considered. The number of layers in the assembly was varied from one to three. In all versions of the calculation, the hold-down clamp was placed in immediate proximity to the edge of the upper blade. The calculations yielded the following maximum shear stresses depending

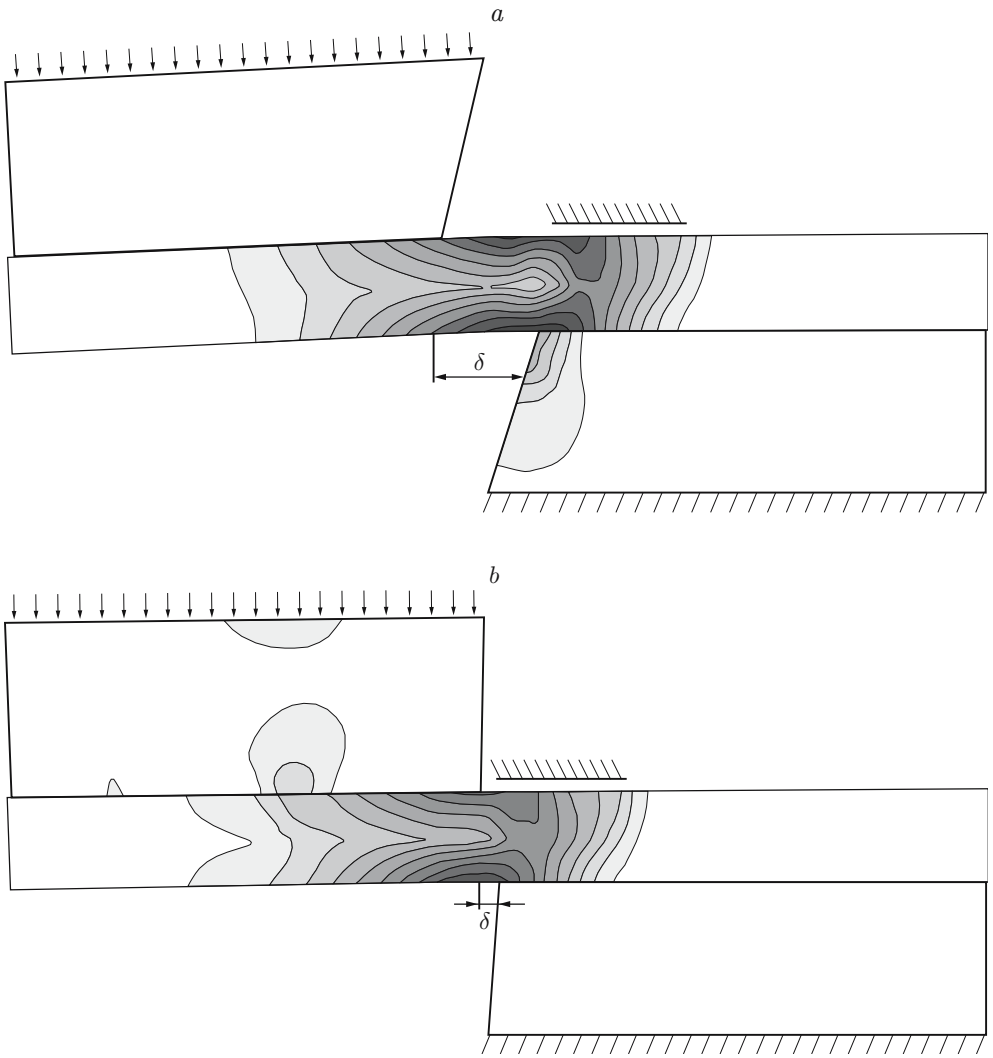

Fig. 5. Shear stress isolines in a single plate for $\delta = 10$ (a) and 2 mm (b).

on the number of layers in the assembly: $(\sigma_i)_a^{\max} = 1850$ MPa for one layer, $(\sigma_i)_a^{\max} = 1950$ MPa for two layers, and $(\sigma_i)_a^{\max} = 2200$ MPa for three layers.

In the case of two- or three-layer assemblies and an external load on the moving blade $P = 150$ MPa, the maximum shear stresses arise in the upper layer and considerably exceed the structural limit of the irradiated material [5]. In the case of a monolithic layer, the maximum shear stresses are minimal. Therefore, the loads necessary for failure decrease with increasing number of layers for unchanged thickness of the assembly.

Conclusions. The results of the numerical calculations lead to the conclusion that the wearing of the blade edges has a weak influence on the shearing effectiveness of the outer layers but considerably reduces the shearing effectiveness of layered materials in the final stage of the process.

The most favorable localization of the hold-down clamp is in immediate proximity to the edge of the moving blade. The conclusions were drawn from analysis of the stress–strained state of the assembly resulting from contact loading. In the analysis, the version in which the stress–strain state corresponded to the greatest extent to pure shear was preferred.

REFERENCES

1. S. P. Timoshenko, *Course in the Theory of Elasticity* [in Russian], Nauk. Dumka (1972).
2. I. M. Belen'kii, *Introduction to Analytical Mechanics* [in Russian], Vysshaya Shkola, Moscow (1964).
3. D. Norrie and G. de Vries, *An Introduction to Finite Element Analysis*, Academic Press, New York (1978).
4. G. Strang and G. Fix, *An Analysis of the Finite Element Method*, Prentice-Hall, Englewood Cliffs (1973).
5. S. N. Ivanov, Yu. V. Konobeev, O. V. Starkov, et al., "Materials science studies of fuel elements irradiated in the Obninsk atomic power plant reactor after a 38-year's storage," *Atom. Énerg.*, **88**, No. 3, 183–188 (2000).